DYNAMIC LIGHT-SCATTERING STUDY ON CHANGES IN FLEXIBILITY OF FILAMENTOUS BACTERIOPHAGE Pf1 WITH TEMPERATURE

SHIGEO SASAKI AND SATORU FUJIME
Mitsubishi-Kasei Institute of Life Sciences, Machida, Tokyo 194, Japan

ABSTRACT The temperature dependence of the flexibility of bacteriophage Pf1 was investigated by dynamic light scattering, and the following results were obtained: (*a*) The $\bar{\Gamma}/K^2$ values measured at 1°–25°C and at various K values were T/η-scaled to 20°C, where $\bar{\Gamma}$ is the first cumulant of the field correlation function of scattered light, K is the length of the scattering vector, T is the absolute temperature, and η is the solvent viscosity at T. And it was found that the scaled $\bar{\Gamma}/K^2$ values at low K values were independent of temperature, whereas those at high K values increased sigmoidally and reversibly against temperature. This suggests that the virion is more flexible at temperatures above the transition temperature T_t. (*b*) This characteristic temperature T_t depended on the pH of the suspension: T_t = 11°C at pH 6.9 and T_t = 8°C at pH 8.2.

INTRODUCTION

Bacteriophage Pf1 is a filamentous and single-stranded phage whose rod-like structure is made up of several thousands of unit coat proteins stacked helically (Makowski, 1984). The single-stranded DNA is covered with a cylindrical shell formed by the coat proteins. Pf1 is known to show a transition in the stacking structure of the coat proteins at a temperature $T_t \sim 8$°C. The symmetry of the Pf1 virion changes slightly with temperature (T) between 4°C and room temperature (Wachtel et al., 1976; Nave et al., 1979). The axial rise per protein subunit changes from 0.304 nm at 4°C to 0.290 nm at room temperature and the number of units per one turn of the basic helix changes from 5.46 to 5.40 with virtually no accompanying change in the structure of the subunit. It is found that the subunit is composed of two α-helices that form inner and outer shells (Makowski et al., 1980; Nakashima et al., 1975). The electron densities from x-ray diffraction data indicate that the α-helical rod in the outer shell tilts by ~22° and 26° relative to the virion axis below and above the transition temperature, respectively, whereas the tilt angle of the inner helical rod is found to be ~6° and little dependent on temperature (Makowski, 1984). These small local changes in structure are amplified over the length of the virion so that during the transition one end of the virion rotates with respect to the other by ~15 turns and the length of the virion changes by ~100 nm.

To detect a change in stacking strength with temperature, the flexibility of Pf1 was examined by using the technique of dynamic light scattering. General background information about dynamic light scattering is found in standard textbooks (Chu, 1974; Berne and Percora, 1975). As we have shown for fd virus (Maeda and Fujime, 1985) and poly(γ-benzyl L-glutamate) in a helicogenic solvent (Kubota et al., 1986), the dynamic light-scattering method is sensitive to probe the apparent flexibility of long and semiflexible filaments.

THEORETICAL BACKGROUND

For a free Brownian motion of a semiflexible rod in suspension, the average decay rate of the time autocorrelation function $G^1(\tau)$ of the electric field of polarized scattered light can be written as (Maeda and Fujime, 1974)

$$\bar{\Gamma}/K^2 = D_0 + (L^2/12)\,\Theta f_1^*(k) + (D_3 - D_1)\,[f_2^*(k) - \tfrac{1}{3}] + (k_B T/4\pi\eta L)\,\Sigma\,(1 + f_m)\,a_m(k), \quad (1)$$

where $D_0 = (2D_1 + D_3)/3$ is the overall translational diffusion coefficient, D_1 and D_3 are, respectively, translational diffusion coefficients perpendicular and parallel to the mean long axis of the rod undergoing bending motions, Θ is the end-over-end rotational diffusion coefficient, K is the length of the scattering vector, and L is the contour

This paper is dedicated to Professor F. Oosawa on the occasion of his retirement from Osaka and Nagoya Universities (1986). As early as 1967, he suggested to one of us (S.Fujime) the feasibility of detecting flexion modes of long and semiflexible scatterers by dynamic light scattering.

Shigeo Sasaki's present address is Mitsubishi-Monsanto Chemical Co., 1 Tohocho, Yokkaichi 510, Japan.

Correspondence should be addressed to Satoru Fujime.

length of the scatterer. $f_i^*(k)$ $(i = 1, 2)$ and $a_m(k)$ $(m \geq 2)$ are functions of only the flexibility parameter (γ) and $k = KL/2$. Since η denotes the viscosity of the solvent and f_m $(m \geq 2)$ denotes the hydrodynamic interaction factor, which depends only on γ, L, and d (diameter), $D_{[m]} = (k_BT/4\pi\eta L)(1 + f_m)$ is the diffusion coefficient for the mth bending mode of the semiflexible rod. Explicit expressions for $f_i^*(k)$ $(i = 1, 2)$, $a_m(k)$, and f_m $(m \geq 2)$ are found elsewhere (Maeda and Fujime, 1984; Fujime and Maeda, 1985; Kubota et al., 1986). The first term in Eq. 1 shows the contribution from translational diffusion, the second term from rotational diffusion, the third term from anisotropy in translational diffusion, and the fourth term(s) from internal bending motion(s). $\bar{\Gamma}/K^2$ tends toward D_0 as $K \to 0$ and toward $D_1 + (L^2/12)\Theta + \Sigma_m D_{[m]}$ as $K \to \infty$. In an accessible range of K values we have $\bar{\Gamma}/K^2$ values between these two limits; the larger the K value is, the larger the $\bar{\Gamma}/K^2$ value is.

Some important predictions of Eq. 1 are: (*a*) The more flexible the rod is, the larger the $\bar{\Gamma}/K^2$ value. For such a very long and semiflexible scatterer as Pf1, this mainly comes from the increasing contribution of the fourth term(s), and partly from the increases in D_0 and Θ and decrease in $(D_3 - D_1)$ with increasing γ. (*b*) Since D_i, Θ, and $D_{[m]}$ are proportional to T/η, $(\bar{\Gamma}/K^2)$ (η/T) at a given K is a function of only γ, L, and d. If the observed $\bar{\Gamma}/K^2$ values at a given K and different temperatures cannot be scaled with T/η, it is concluded that the nonzero flexibility parameter γ (the inverse of the Kuhn length) depends on temperature under the assumption of no changes in the size parameters (L and d) (Fujime and Maeda, 1982).

METHODS

Pf1 Sample

Pf1 phage was kindly provided by Professor D. L. D. Caspar of Brandeis University. Electron microscopic observations showed that the length distribution of this phage had a sharp peak at its intact length of $L \simeq 2$ μm and a broad peak centered at $L \simeq 1$ μm (Fig. 1). The latter peak suggested that about one-half of phage particles once encountered single breaking, resulting in a binomial-like distribution in length. This breaking is probably due to the shear force exerted on thin phage particles ($d = 6$ nm) during transportation of the sample. Unfortunately, the polydispersity of the sample prevented us from making a very quantitative analysis of the experimental results, but as shown below, we could extract some qualitative but distinct information about the structural changes of Pf1 with temperature.

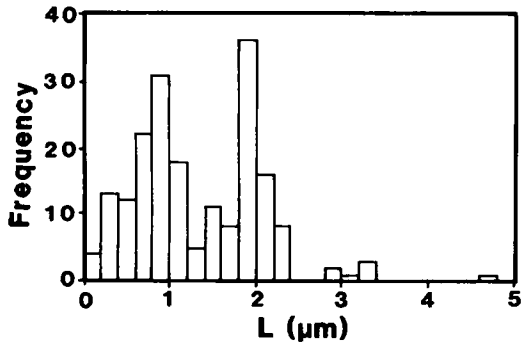

FIGURE 1 The length distribution of Pf1 particles used in the experiments. This histogram was obtained from electron micrographs.

Since our Pf1 samples were not originally prepared for light-scattering experiments, dust that remained in suspensions was a serious problem. Because of a limited amount of the sample, we did not perform any special procedure to remove dust; we only used simple centrifugation. Two-thirds of the supernatant of the phage suspension, centrifuged at 4,000 *g* for 12 h, were carefully taken and transferred into a 10-mm outer diameter scattering cell, which had been rinsed several times with dust-free water, and just before light-scattering measurements, the sample suspension in the scattering cell was again centrifuged at 4,000 *g* for several hours. The phage concentration in the scattering cell was determined by a uv absorption measurement after light-scattering experiments.

Light-Scattering

Dynamic light-scattering measurements were carried out by using a conventional apparatus described elsewhere (Fujime et al., 1984). We used a 488-nm beam from an Ar^+ laser as a light source. Light-scattering measurements were made over a temperature range of 1°–25°C and a scattering angle range of 20°–140° (or of 0.595×10^5 to 3.22×10^5 cm^{-1} in K). The homodyne intensity autocorrelation function $G^2(\tau)$ is related to the normalized field correlation function $g^1(\tau) \equiv G^1(\tau)/G^1(0)$ by $G^2(\tau) = B(1 + \beta|g^1(\tau)|^2)$, where B is the baseline, β is a machine constant, and τ is the delay time ($\tau = n\Delta\tau$, n is the channel number, and $\Delta\tau$ is the channel width). The third-order nonlinear cumulant expansion was adopted to obtain the first cumulant $\bar{\Gamma}$ in Eq. 1 (Koppel, 1972).

Proper choice of the sampling time $\Delta\tau$ was very important in our case where temperature and/or K values were widely varied (see Appendix). From Eq. 1 we know $\bar{\Gamma} \propto (T/\eta)K^2$, so that $(T/\eta)K^2\Delta\tau$ should be kept constant throughout experiments at different temperatures and/or K values. Since our correlator had 128 channels, $\Delta\tau$ at a scattering angle of 90° and a temperature of 20°C was first determined so that $G^1(100\Delta\tau)/G^1(\Delta\tau) \sim 0.05$. Then, $\Delta\tau$ for other temperatures and/or K values was determined so as to keep $(T/\eta)K^2\Delta\tau$ constant. In the following, $\bar{\Gamma}$ values measured at temperature T will be displayed in terms of the apparent diffusion coefficient corrected to 20°C: $D_{app}^{20} = (\bar{\Gamma}/K^2)(\eta_T/\eta_{293})(293/T)$ with T in Kelvin units.

RESULTS AND DISCUSSION

Fig. 2 shows the results at pH 6.9. D_{app}^{20} at $K = 2.42 \times 10^5$ cm^{-1} (*solid circles*) increased with temperature gradually up to ~9°C and rapidly in a range 9°–12°C, and above 12°C it stayed essentially the same value. This change in D_{app}^{20} was reversible; no appreciable hysteresis was observed on heating and cooling. The transition temperature T_t determined from the midpoint of the change in D_{app}^{20} was ~11°C at this pH.

To discuss D_{app}^{20} vs. K relationships at 20.8°C (*open circles*) and at 1.5°C (*open squares*), Fig. 2 shows the theoretical predictions of D_{app}^{20} for a rigid rod (*solid lines*) and a semiflexible rod (*dashed lines*), where M is for the monodisperse distribution with $L = 1.90$ μm and the hydrodynamic effective diameter of $d = 7.0$ nm, and P is for the observed polydisperse distribution shown in Fig. 1 (see Appendix). We tentatively assumed a γ value appropriate to fd virus (Maeda and Fujime, 1985). At the lowest K $(= 0.595 \times 10^5$ $cm^{-1})$, partial heterodyning occurred and scattering from dusts might contribute to the spectrum, so that experimental D_{app}^{20} at this K might be smaller

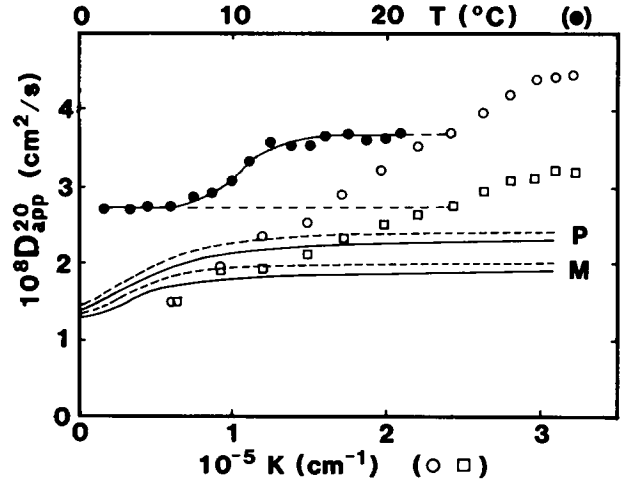

FIGURE 2 D_{app}^{20} vs. K at 20.8°C (*open circles*) and 1.5°C (*open squares*), and D_{app}^{20} vs. T(°C) at the scattering angle of 90° or $K = 2.42 \times 10^5$ cm^{-1} (*solid circles*) for a suspension of 0.10_5 mg/ml Pf1 in 0.3 M KCl and 0.1 M phosphate buffer at pH 6.9. The standard deviation of each point is a little larger than the size of each symbol. The solid lines show the theoretical D_{app}^{20} for a rigid rod and the dashed lines for a semiflexible rod based on Eq. 1 without $a_m(k)$ terms. *M* stands for monodisperse and *P* for polydisperse. For details, see Appendix.

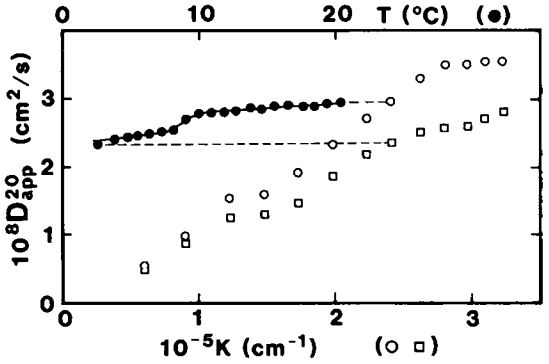

FIGURE 3 D_{app}^{20} vs. K at 20.3°C (*open circles*) and 2.5°C (*open squares*), and D_{app}^{20} vs. T(°C) at the scattering angle of 90° or $K = 2.42 \times 10^5$ cm^{-1} (*solid circles*) for a suspension of 0.10_5 mg/ml Pf1 in 0.3 M KCl and 0.1 M Tris-HCl at pH 8.2. The standard deviation of each point is a little larger than the size of each symbol.

than the true ones. If we take this situation into account, D_{app}^{20} extrapolated to $K = 0$ will be close to D_0 (rigid rod, *M*) = 1.31, D_0 (rigid rod, *P*) = 1.38, D_0 (semiflexible, *M*) = 1.35, and D_0 (semiflexible, *P*) = 1.43 in units of 10^{-8} cm^2/s. Even at the lowest K, contributions from the second and the third terms in Eq. 1 are estimated to have almost saturation values (Fig. 5 in Appendix), so that an increase in D_{app}^{20} with K at both temperatures is due to the increasing contribution(s) from the fourth term(s) with K. At the lowest two K values, D_{app}^{20} for both temperatures coincide with each other within experimental error. (At the lowest K, D_{app}^{20} might be affected by partial heterodyning and scattering from dust, but this does not matter for the discussion about T/η-scaling of D_{app}^{20}). As K increases, on the other hand, the difference between D_{app}^{20} values at two temperatures increases; namely, T/ηscaling does not hold except for very low K values.

The data at low K values and the reversibility in the change of D_{app}^{20} with temperature suggest that the average length and the length distribution of Pf1 in our suspension are the same for both temperatures. Then, data at high K values suggest that the Pf1 is more flexible at 20.8°C (*open circles*) than at 1.5°C (*open squares*). D_{app}^{20} at a given K is an increasing function of γ, but it is not directly proportional to γ. Then, the dependence on temperature of D_{app}^{20} (*solid circles*) approximately traces that of the flexibility change of Pf1, but the transition temperature T_t from D_{app}^{20} given above may or may not be the same as that from the flexibility itself (γ) and also as that from data by other techniques.

Essentially similar results were obtained at pH 8.2 (Fig. 3) as at pH 6.9. Just after the preparation of the scattering sample at this pH, D_{app}^{20} at a temperature of 20°C and a scattering angle of 90° was very close to that at pH 6.9, but it became small with time. The reason for this is not clear, but it is inferred that a kind of aggregation gradually occurred at this pH. The results in Fig. 3 were obtained a couple of days after the preparation of the scattering sample, and D_{app}^{20} at any temperature and/or K value is smaller than the corresponding one at pH 6.9. Although the quality of the data at pH 8.2 is not good compared with that at pH 6.9, the transitional change in the filament flexibility can also be clearly seen at pH 8.2. The transition temperature T_t at pH 8.2 was ~8°C.

As an additional experiment, variation of circular dichroism with temperature was examined (data not shown). The fractional change in the measurement with temperature showed the midpoint at ~15°C for both pH 6.9 and 8.2. This temperature T_t was the same as that in the previous report (Hinz et al., 1980).

Although no quantitative analysis of experimental results has been made, our data clearly indicate the transitional increase in the flexibility of Pf1 with temperature. As discussed in the Appendix, the high temperature form of Pf1 is inferred to have the flexibility parameter nearly equal to that of fd, and the low temperature form of Pf1 is a little stiffer than the high temperature form. The small local changes in structure of the virion are amplified over the length of the virion, so that the change in the overall flexibility was easily probed by dynamic light scattering. The increase in the overall flexibility with temperture might be a reflection of the decrease in the strength of stacking forces among protein units. Our conclusion is consistent with the previous report that from specific heat measurements, the low temperature form of the virion at 0°C is found to be stabilized by ~0.9 kJ (mol protein)$^{-1}$ in the Gibbs free energy relative to the high temperature form at 25°C (Hinz et al., 1980).

It has been known that Pf1 is very resistive to pH (Makowski, 1984). However, our light-scattering results

clearly showed the pH dependence of the structural transition of Pf1. It is possible (but not conclusive) that an ionizable residue(s) such as aspartic acid in the protein unit is ionized at higher pH so that the stacking structure is destabilized to some extent, resulting in a lower transition temperature at pH 8.2 than at pH 6.9, without any shift in the fractional change in circular dichroism (without an appreciable change in the environment of the tyrosine residues responsible for circular dichroism).

APPENDIX

General Remarks

For cases where the sample is polydisperse and various motions other than translation strongly contribute to the light-scattering spectrum, the field correlation function is highly non-exponential and its first cumulant strongly depends on the sampling time $\Delta\tau$ for a given number of the channels of the correlator or on the number of the channels for a given sampling time. Fig. 4 shows an example of $|g^1(n\Delta\tau)|^2$ at $\Delta\tau = 20$ μs, a temperture of 20°C, and a scattering angle of 90°. As shown in the inset (*solid circles*) of Fig. 4, D_{app}^{20} values strongly depend on the last channel number in the cumulant analysis. Because of this, we adopted a criterion mentioned in Methods section for the choice of the sampling time at a given temperature and/or K.

Other remarks are as follows: For a given $\Delta\tau$, contributions to the correlation function from decay modes with decay times shorter than several multiple of $\Delta\tau$ cannot be detected experimentally. Our choice of $\Delta\tau$ seems to be rather long as seen from the profile of the correlation function shown in Fig. 4. However, the following estimation will provide us assertion to our procedure. (We tentatively assume the γ value appropriate to fd virus [Maeda and Fujime, 1985], i.e., $\gamma L = 0.23$ for fd [$L = 0.895$ μm] or $\gamma L = 0.49$ for Pf1 [$L = 1.90$ μm]). The relaxation time τ_m of the mth bending mode is given by $\tau_m = [2\gamma L^3/(\beta_m L)^4]/D_{[m]}$, where β_m is the eigenvalue. For Pf1 with $L = 1.90$ μm and $d = 7.0$ nm (monodisperse), we have $\tau_m \simeq$ 9,200, 1,300, 350, and 140 [μs] for $m = 2$, 3, 4, and 5, respectively. The sampling time of $\Delta\tau = 20$ μs at the scattering angle of 90°, for example, is short enough to detect the internal modes up to $m = 4$, if their amplitudes are appreciably large. On the other hand, the sampling time of $\Delta\tau = 270$ μs at a scattering angle of 30° is short enough to detect only the $m = 2$ mode even if other modes have appreciable amplitudes.

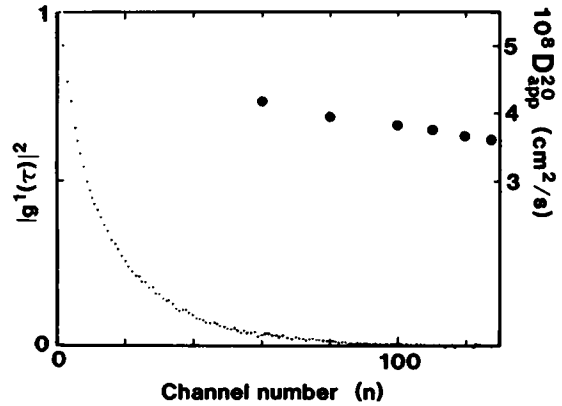

FIGURE 4 An example of $|g^1(n\Delta\tau)|^2$ of a suspension of Pf1 at 0.10$_3$ mg/ml and pH 6.9. Temperature, 20°C; $\Delta\tau$, 20 μs; scattering angle, 90°. In this plot, the first point ($n = 1$) is simply normalized to unity. The inset shows D_{app}^{20} obtained by cumulant expansion of the correlation function from $n = 1$ to 60, 80, 100, 110, 120, and 128.

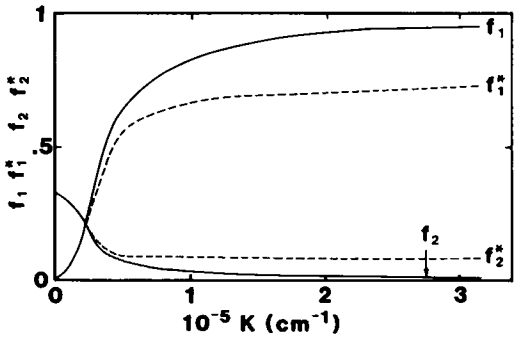

FIGURE 5 Graphic representation of functions $f_1(k)$ and $f_2(k)$ for a rigid rod and $f_1^*(k)$ and $f_2^*(k)$ for a semiflexible rod with $\gamma L = 0.49$, $L = 1.90$ μm, and $d = 7.0$ nm. For details, see Appendix.

On Average Over Length Distribution

For a length distribution function $W(L)$, the light-scattering z-average $\langle f(L)\rangle_z$ of a quantity $f(L)$ is defined by

$$\langle f(L)\rangle_z = \int f(L)P(k)L^2W(L)\,dL / \int P(k)L^2W(L)\,dL, \quad \text{(A1)}$$

where $P(k)$ is the scattering function. Since $P(k)$ tends toward unity as $k \to 0$, the z-average of $f(L)$ at $K = 0$, $\langle f(L)\rangle_z^0$, is easily computed, where the superscript 0 stands for the quantity at $K = 0$. By use of Eq. A1 with $P(k) = 1$ and $W(L)$ in Fig. 1, $\langle D_0\rangle_z^0$ for a rigid rod and a semiflexible filament are computed and given in the text as D_0 (rigid rod, P) and D_0 (semiflexible, P). To compute $\langle \bar{\Gamma}/K^2\rangle_z$ for a rigid rod, an argorithm for computation of the dynamic form factor (Fujime and Kubota, 1985) and an argorithm for computation of $\langle D_0 - (D_3 - D_1)/3\rangle_z \equiv \langle D_1\rangle_z$, $\langle L^2\Theta f_1(k)\rangle_z$ and $\langle (D_3 - D_1)f_2(k)\rangle_z$ (Kubota et al., 1985) are useful. The computed result for $W(L)$ in Fig. 1 is given in Fig. 2 (*solid line* with label P). Computation of $\langle \bar{\Gamma}/K^2\rangle_z$ for a semiflexible rod is essentially the same as that for a rigid rod given above. The required threefold integration was numerically carried out on a minicomputer (Eclipse S-140; Nippon Data General, Tokyo) by use of a subroutine ADAPT: an adaptive multidimensional quadrature subroutine (Maeda and Fujime, 1985). Fig. 5 shows $f_1(k)$ and $f_2(k)$ for a rigid rod (*solid lines*), and $f_1^*(k)$ and $f_2^*(k)$ for a semiflexible rod with $\gamma L = 0.49$ (*dashed lines*), where the size parameters of $L = 1.90$ μm and $d = 7.0$ nm were assumed for both cases. By computation of $f_1^*(k)$ and $f_2^*(k)$ for various values of K and L, we finally obtained the z-average of Eq. 1 without the fourth terms(s) for a suspension of semiflexible rods with the polydispersity shown in Fig. 1, and the result is shown in Fig. 2 by the dashed line with label P.

On Internal Bending Motions

Large deviations of experimental points (*open circles, open squares*) at large K from theoretical curves with label P in Fig. 2 come from the large contribution(s) of the fourth term(s) in Eq. 1. How many modes should be taken into account to estimate the contribution from the fourth term(s) in Eq. 1? A criterion for this has been discussed; those modes that satisfy $\tau_m > 10\,\Delta\tau$, for example, should be taken into account. Another criterion will be that the root-mean-square amplitude of the mth bending motion, $\langle \delta_m^2\rangle^{1/2}$, should not be very smaller than $1/K$. The relation $\langle \delta_m^2\rangle = 2D_{[m]}\tau_m$ gives $\langle \delta_m^2\rangle^{1/2} \simeq$ 120, 43, 22, and 13 [nm] again for $L = 1.90$ μm and $\gamma L = 0.49$. Comparing these values with $1/K = 41$ nm at the scattering angle of 90°, we can expect to detect the internal modes of $m = 2$, 3 and probably 4 at this angle (but only the $m = 2$ mode at the scattering angle of 30° for which $1/K = 110$ nm). We also estimate $D_{[m]} \simeq$ 0.77, 0.72, and 0.68 [$\times 10^{-8}$ cm^2/s] for $m = 2$, 3, and 4, respectively. Then, we have $a_2(k)D_{[2]} + a_3(k)D_{[3]}$ $(+a_4(k)D_{[4]}) = 0.74 \times 0.77 + 0.74 \times 0.72$ $(+0.74 \times 0.68) = 1.1$ $(+0.5)$ in units of 10^{-8} cm^2/s at the scattering angle of 90°. (At this angle $a_m(k)$ for $m = 2$, 3, and 4 have the value of 0.74). This value of 1.1×10^{-8} cm^2/s (or 1.6×10^{-8} cm^2/s) is

large enough to explain the excess value of the experimental point (*open circles*) at the scattering angle of 90° from the theoretical lines with label *P* in Fig. 2. The data (*solid circles*) in Fig. 2 can then be qualitatively interpreted that Pf1 has a flexibility nearly equal to fd at temperatures higher than T_t and that Pf1 is less flexible at temperatures below T_t.

We thank Professors D. L. D. Caspar of Brandeis University and S. Asakura of Nagoya University for suggesting us to study Pf1 by dynamic light scattering. We also thank Mr. S. Kondo for his kind advice in electron microscopy. Advice of Dr. T. Maeda in our use of his subroutine ADAPT and technical assistance of Mrs. M. Takasaki-Ohsita were very helpful in machine computation given in Appendix.

S. Sasaki thanks the postdoctoral fellowship (March 1985 to February 1986) from this Institute. This work was partly supported by a Grant-in-Aid from the Ministry of Education, Science and Culture of Japan.

Received for publication 9 June 1986 and in final form 8 September 1986.

REFERENCES

Berne, B., and R. Pecora. 1975. Dynamic Light Scattering. Interscience, New York. 376 pp.

Chu, B. 1974. Laser Light Scattering. Academic Press, Inc., New York. 317 pp.

Fujime, S., and T. Maeda. 1982. A note on T/η-scaling of dynamic light-scattering spectrum. *Biophys. J.* 38:213.

Fujime, S., S. Ishiwata, and T. Maeda. 1984. Dynamic light scattering study of muscle F-actin. *Biophys. Chem.* 20:1–21.

Fujime, S., and K. Kubota. 1985. Dynamic light scattering from dilute suspensions of thin discs and thin rods as limiting forms of cylinder, ellipsoid and ellipsoidal shell of revolution. *Biophys. Chem.* 23:1–13.

Fujime, S., and T. Maeda. 1985. Spectrum of light quasi-elastically scattered from dilute solutions of very long and slightly bendable rods. Effect of hydrodynamic interaction. *Macromolecules.* 18:191–195.

Hinz, H. J., K. O. Greulich, H. Ludwig, and D. A. Marvin. 1980. Calorimetric, density and circular dichroism studies of the reversible structural transition in Pf1 filamentous bacterial virus. *J. Mol. Biol.* 144:281–289.

Koppel, D. E. 1972. Analysis of macromolecular polydispersity in intensity correlation spectroscopy: the method of cumulant. *J. Chem. Phys.* 57:4814–4820.

Kubota, K., Y. Tominaga, S. Fujime, J. Otomo, and A. Ikegami. 1985. Dynamic light scattering study of suspensions of purple membrane. *Biophys. Chem.* 23:15–29.

Kubota, K., Y. Tominaga, and S. Fujime. 1986. Quasielastic light-scattering study of semiflexible polymers. Poly(γ-benzyl L-glutamate) in dimethylformamide. *Macromolecules.* 19:139–144.

Maeda, T., and S. Fujime. 1984. Spectrum of light quasielastically scattered from solutions of semiflexible filaments in the dilute and semidilute regimes. *Macromolecules.* 17:2381–2391.

Maeda, T., and S. Fujime. 1985. Dynamic light-scattering study of suspensions of fd virus. Application of a theory of the light-scattering spectrum of weakly bending filaments. *Macromolecules.* 18:2430–2437.

Makowski, L. 1984. Biological Macromolecules and Assemblies. I. Virus Structures. A. Jurnak and A. McPherson, editors. John Wiley & Sons, Inc., New York. 203–253.

Makowski, L., D. L. D. Caspar, and D. A. Marvin. 1980. Filamentous bacteriophage Pf1 structure determined at 7 Å resolution by refinement of models for the α-helical subunit. *J. Mol. Biol.* 140:149–181.

Nakashima, Y., R. L. Wiseman, W. Konigsberg, and D. A. Marvin. 1975. Primary structure and sidechain interactions of Pf1 filamentaous bacterial virus coat protein. *Nature (Lond.).* 253:68–71.

Nave, C., A. G. Fowler, S. Malsey, D. A. Marvin, H. Siegrist, and E. J. Wachtel. 1979. Macromolecular structural transitions in Pf1 filamentous bacterial virus. *Nature (Lond.).* 281:232–234.

Wachtel, E. J., F. J. Marvin, and D. A. Marvin. 1976. Structural transition in a filamentous protein. *J. Mol. Biol.* 107:379–383.